

# NUMERICAL SIMULATION OF OIL LEAKAGE, WATER FLOODING AND DAMAGED STABILITY OF OIL CARRIER BASED ON MOVING PARTICLE SEMI-IMPLICIT (MPS) METHOD

LIANG-YEE CHENG<sup>\*</sup>, DIOGO V. GOMES<sup>†</sup> ADRIANO M. YOSHINO<sup>†</sup> AND  
KAZUO NISHIMOTO<sup>†</sup>

<sup>\*</sup> Dept. Construction Engineering, Escola Politécnica  
University of São Paulo  
Av. Almeida Prado, Trav. 2 No. 83, Ed. Engenharia Civil, 05508-900 São Paulo, SP, Brazil  
e-mail: cheng.yee@poli.usp.br, web page: <http://www.pcc.usp.br>  
e-mail: diogo.gomes@usp.br, web page: <http://www.pcc.usp.br>  
e-mail: yoshino@usp.br, web page: <http://www.pcc.usp.br>

<sup>†</sup> Dept. Naval Engineering Naval Architecture and Ocean Engineering, Escola Politécnica  
University of São Paulo  
Av. Professor Melo Moraes, 2231, 05508-900 São Paulo, SP, Brazil  
e-mail: knishimo@usp.br, web page: <http://tpn.usp.br>

**Key words:** Moving Particle Semi-Implicit, MPS, multiphase flow, oil leakage, water flooding, damaged stability.

**Abstract.** Oil leakage or water flooding in a damaged oil carrier are complex phenomena that involve fluid-solid interaction with complicated geometry and multiphase flow. In order to assess the damaged stability and environmental impact when the damage occurs, the present research models the non-linear hydrodynamic problems by using a numerical approach based on MPS (Moving particle Semi-Implicit) method. The comparison of numerical results with that obtained by quasi-static approach shows the limit of validity of the last one. Considering the reduced dimension of the opening of the damage, the effects of the resolution of spatial discretization are also analysed.

## 1 INTRODUCTION

Oil leakage or water flooding in case of damage are of great concern in the design and operation of crude oil carriers due to the safety and the environmental issues. Due to the fluid-solid interaction with complex geometry and multiphase flow, the detailed investigation of the phenomena, including the coupled transient motions of the fluids and the hull, still remains as a challenge.

Within this context, the objective of the present research is to carry out a coupled transient analysis of the oil leakage and water flooding processes and to determine the final list angles and oil leak or water flooding volumes. In order to model both the motion of the vessel and the oil-water multiphase flow with free surface, a numerical approach based on MPS (Moving particle Semi-Implicit) method [1] was adopted. On the other hand, for the surface tension in

the free surface and in the oil -water interface, as well as the wettability of the solid surfaces, a inter-particle potential force model was used [2].

For sake of simplicity, a two dimensional small scaled model and still water condition were considered and the results were compared with that obtained by the stability analysis software SSTAB, which provides the final list angle in case of the damage.

In the previous works [3,4], the dynamics of the oil leakage and water flooding process were analysed taking into account several loading conditions and heights of damage opening. The modelling of the towing tank was also improved to reduce the undesirable effects of wave reflection from the side wall of the tank to achieve more stable and accurate transient behaviours. Nevertheless, in the cases where the volume of leakage or flooding is small, the concern about the accuracy of the particle modelling still remains. This concern is especially important because of the inter-particle potential force approach that may require a higher resolution of the spatial discretization to model the oil -water interface. In this way, beside the analyses on new loading conditions, one of the objective of the present paper is to identify the situations where the spatial resolution might be relevant to improve the accuracy of the numerical results.

## 2 NUMERICAL METHOD

The governing equations for the incompressible viscous flow to be solved in this study are:  
Continuity equation

$$\frac{D\rho}{Dt} = -\rho(\nabla \cdot \vec{u}) = 0 \quad (1)$$

and the momentum equation

$$\frac{D\vec{u}}{Dt} = -\frac{1}{\rho}\nabla P + \nu\nabla^2\vec{u} + \vec{g} + \frac{\vec{\sigma}}{\rho} \quad (2)$$

Where,  $\rho$  is density,  $\vec{u}$  is velocity,  $p$  is pressure,  $\nu$  is kinematic viscosity,  $\vec{\sigma}$  is surface tension and  $\vec{g}$  the gravity.

The Moving Particle Semi-implicit (MPS) is a Lagrangian meshless method, in which the space domain is discretized in particles, and all the differential operators are obtained from a particle interaction model based on the weight function that might be given by:

$$w(r) = \begin{cases} \frac{r_e}{r} - 1, & (r < r_e) \\ 0, & (r > r_e) \end{cases} \quad (3)$$

Where,  $r$  is the distance between two particles and  $r_e$  is the effective radius, which limits the region where the interaction between particles occurs.

Considering a scalar function  $\phi$ , the gradient vector and the Laplacian of the function at a particle  $i$  are determined by taken into account the values of the neighboring particles  $j$ . Within the range  $r_e$ , they are given by Eq. (4) and (5), respectively:

$$\langle \phi \rangle_i = \frac{d}{pnd^0} \sum_{i \neq j} \left[ \frac{(\phi_j - \phi_i)}{|\vec{r}_j - \vec{r}_i|^2} (\vec{r}_j - \vec{r}_i) w(|\vec{r}_j - \vec{r}_i|) \right] \quad (4)$$

$$\langle \nabla^2 \phi \rangle_i = \frac{2d}{pnd^0 \lambda} \sum_{i \neq j} [(\phi_j - \phi_i) w(|\vec{r}_j - \vec{r}_i|)] \quad (5)$$

Where,  $d$  is the number of spatial dimensions,  $pnd$  is the particle number density,  $\vec{r}_i$  and  $\vec{r}_j$  are, respectively, the position vector of particles  $i$  and its neighbor particle  $j$ .  $\lambda$  is calculated by:

$$\lambda = \frac{\sum_{i \neq j} |\vec{r}_j - \vec{r}_i|^2 w(|\vec{r}_j - \vec{r}_i|)}{\sum_{i \neq j} w(|\vec{r}_j - \vec{r}_i|)} \quad (6)$$

Particle number density ( $pnd$ ) is proportional to the fluid density and it is given by:

$$pnd = \sum_{i \neq j} w(|\vec{r}_j - \vec{r}_i|) \quad (7)$$

and  $pnd^0$  is the initial value of  $pnd$ .

The MPS method adopts a semi-implicit algorithm. Except the pressure gradient term, the terms in the right side of Navier-Stokes equation are calculated explicitly to estimate velocity and position. After that, the Poisson's equation of pressure is solved implicitly at  $(t + \Delta t)$ . The Poisson's equation is given by:

$$\langle \nabla^2 P \rangle_i^{t+\Delta t} = -\frac{\rho}{\Delta t^2} \frac{pnd_i^* - pnd^0}{pnd^0} \quad (8)$$

Where,  $pnd^*$  is the particle number density obtained from the particle position estimated explicitly.  $pnd^*$  is kept as  $pnd^0$  to ensure the condition of incompressibility. The term of the left hand side of equation (8) can be discretized using the Laplacian model, leading to a system of linear equations.

For the present two-dimensional analysis,  $r_e$  was set to  $2.1 l_0$ , where  $l_0$  is the initial distance between particles, to calculate pressure gradient and the particle number density.  $r_e$  is set to be  $4.0 l_0$  for cases involving the Laplacian operator.

When the particle number density of a particle is smaller than  $\beta \cdot pnd$ , it is considered to be on the free surface. The pressure of all free surface particles is set to zero. According to Koshizuka and Oka [1],  $\beta$  may vary between 0.80 and 0.99.

For the calculation of the surface tension  $\vec{\sigma}$  on the free surface and at the oil- water interface, the approach proposed by Kondo et al [2] is adopted. According to the proposal of

Kondo et al [2], the surface tension, which is originated from the intermolecular forces, can be approximated by an inter-particle potential force model whose function is give by:

$$P(r) = C \cdot p(r) \quad (9)$$

where  $C$  is a coefficient that defines the intensity of the inter-particle potential, and  $p(r)$  is the shape function of the potential given by:

$$p(r) = \frac{1}{3} \left( r - \frac{3}{2} r_{\min} + \frac{1}{2} r_e \right) (r - r_e)^2 \quad (10)$$

The coefficient  $C$  is obtained from the energy required to form free surfaces when particles from a domain  $A$  separate from their neighbor of another domain  $B$ .

$$C = 2 \frac{r_{\min}^2}{\sum_{i \in A, j \in B} p(r_{i,j})} \sigma \quad (11)$$

Finally, the force due to surface tension is determined from the spatial derivative of the potential:

$$\frac{dP(r)}{dr} = C(r - r_{\min})(r - r_e) \quad (12)$$

In MPS, rows of different type of particles are used to describe the geometry of the rigid walls. Pressure is calculated in the first row that is in contact with fluids. The rows of particles that have no contact with fluids are formed by dummy particles used to guarantee the correct calculation of the particle number density, but in which the calculation of pressure is not necessary.

In case of the floating body with inner tank analyzed in the present study, as the calculation of the liquid pressure on the outside of the hull must not affect the calculation of the pressure inside the hull, and vice-versa, for  $r_e$  equals to  $2.1 l_0$ , it is necessary put at least two rows of dummy particles between the rows of pressure particles that define the geometry of the hull and the inner tank, as shown in Figure 1.

Force and moment acting on the hull are calculated by integrating the pressure on both external and internal sides of the body. The elementary area of the wall is defined as the half distance between a hull particle and one of its neighbor particles. Each area has its normal orienting to the fluid side. Figure 2 shows an example of hull particles, their elementary areas and normal vectors.

The force on the hull and the moment applied at the center of gravity are as follows:

$$F = \sum_i p_i \cdot (S_{i1} \cdot \vec{n}_{i1} + S_{i2} \cdot \vec{n}_{i2})$$

$$M = \sum_i p_i \cdot (S_{i1} \cdot \vec{n}_{i1} + S_{i2} \cdot \vec{n}_{i2}) \times (\vec{r}_i - \vec{r}_{CG}) \quad (13)$$

Where,  $s_{i1}$  and  $s_{i2}$  are the dimension of the two elementary areas of particle  $i$ ;  $p_i$  is the pressure of particle  $i$ ;  $\vec{n}_{i1}$  and  $\vec{n}_{i2}$  are the normal vectors of  $s_{i1}$  and  $s_{i2}$ , respectively, and  $\vec{r}_{CG}$

is the position vector of center of gravity of the floating body.

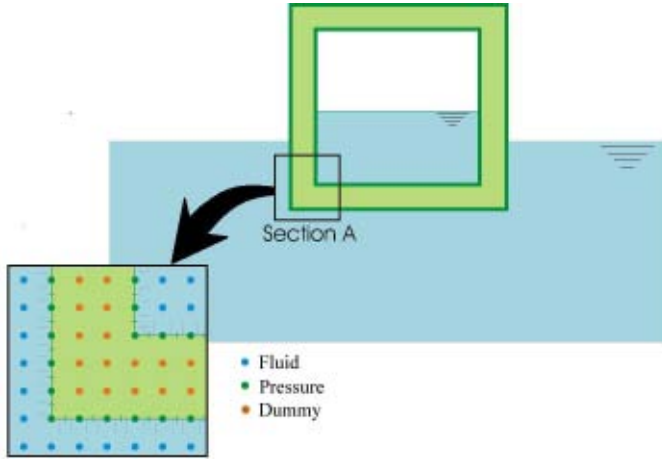


**Figure 1:** Modeling of a hull with internal tank

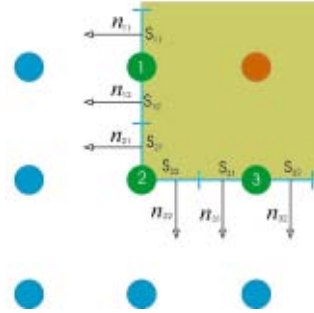


**Figure 2:** Elementary area and normal vector

With the force and the moment calculated by equations (13), the dynamics of the floating body can be obtained by:

$$\begin{aligned}
 m \frac{d^2 \vec{r}_{CG}}{dt^2} &= F \\
 I \frac{d^2 \vec{\theta}}{dt^2} &= M
 \end{aligned}
 \tag{14}$$

where,  $m$  and  $I$  are mass and inertia of rigid body respectively;  $\theta$  is the roll angle.

### 3 CASES OF STUDY

To investigate the oil leakage or water flooding processes in a damaged oil carrier, a 2D numerical scaled model was used. The main characteristics of the model are described in Table 1.

**Table 1:** The main properties of the hull.

Property	Without ballast (B0)	With ballast (B15)
Beam (m)	0.415	0.415
Depth (m)	0.325	0.325
Mass (kg/m)	25.109	40.109
Inertia (Kgm <sup>2</sup> /m)	0.801	1.088
TCG (m)	0.0	0.0
VCG (m)	0.129	0.094

The scaled model has two internal tanks. The thickness of the walls is 0.02 m except in center, where the thickness is 0.025 m, and in the bottom, where the thickness of 0.055 m is used to model the double bottom. The opening for the oil leakage is 0.05 m. In the case shown in Figure 3, the opening height is 0.20 m from the keel, and the filling ratio of the internal tank is 75%.

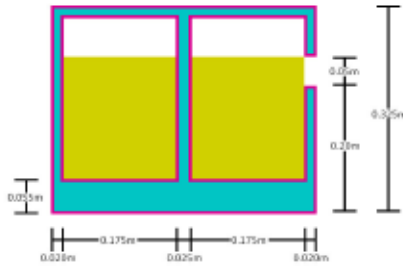


**Figure 3:** Cross-section of the model showing the opening height of 0.20 m from the keel, and 75% filling

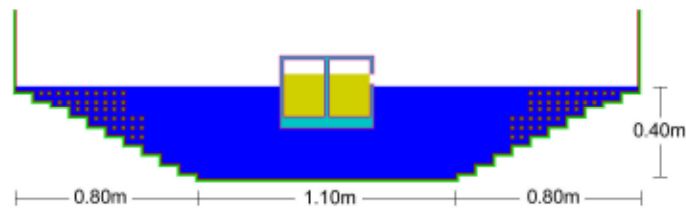


**Figure 4:** Dimensions of the towing tank

The total width of the towing tank used in the numerical simulations is 2.7 m, as shown in Figure 4. In order to minimize the reflection of waves generated by the dynamic motion of the hull, beaches of 0.8 m are modeled in both extremity of the towing tank. The slope of the beaches is approximately 30 degrees. Squares of 3x3 particles are fixed close to the beaches. The depth of the towing tank used in the simulation is 0.40 m.

Table 2 gives the nomenclature of the cases analyzed in the present study. Three different location of damage and three levels of filling inside the tanks were considered. Due to the concern about the accuracy of the particle modelling, simulations with two levels of spatial discretization were performed for each case listed in Table 2: low and high resolutions. The simulations with low resolution were carried out by using distance between particles of 0.0050 m and there are about 34000 particles in a typical case, as in the previous works [3,4]. On the other hand, the simulations with high resolution were performed using distance between particles of 0.0025 m with near to 140000 particles in a typical case. The time step was 0.0005 s and simulation times up to 10.0 s were used.

The properties of the water and the oil are given in Table 3.

**Table 2:** The cases of study.

Case denomination	Filling ratio (%)	Damage height above the keel (m)
B0_75%_020	75	0.20
B0_75%_014	75	0.14
B0_75%_010	75	0.10
B0_45%_014	45	0.14
B0_45%_010	45	0.10
B0_25%_010	25	0.10

**Table 3:** The properties of the water and oil.

Property	Water	Oil
Density ( $\text{kg/m}^3$ )	1000.0	900.0
Viscosity ( $\text{m}^2/\text{s}$ )	$1.0 \times 10^{-6}$	$5.0 \times 10^{-5}$
Surface Tension Coefficient (N/m)	0.072	0.026

#### 4 RESULTS AND DISCUSSIONS

Figure 5 gives the snapshots of the animation obtained from the MPS simulation with 75% filling and opening at 0.10 m above the keel (B0\_75%\_010). Owing to large vertical distance from oil level to opening position, where the internal oil pressure higher than external water one, this is the case in which large oil leak is expected together with more violent transient motions. Actually, the transient analysis performed by the present study shows that a list angle nearly  $30^\circ$  degrees is reached in about 2 seconds after the breakdown. Also, beside the roll motion of the hull, drift motion induced by the leakage occurs in the beginning of the process when a relatively large volume of the oil is released suddenly. The comparison between Figure 5(a) and Figure 5(b) shows that the higher spatial resolution gives more detail description of the oil flow outside of the hull.

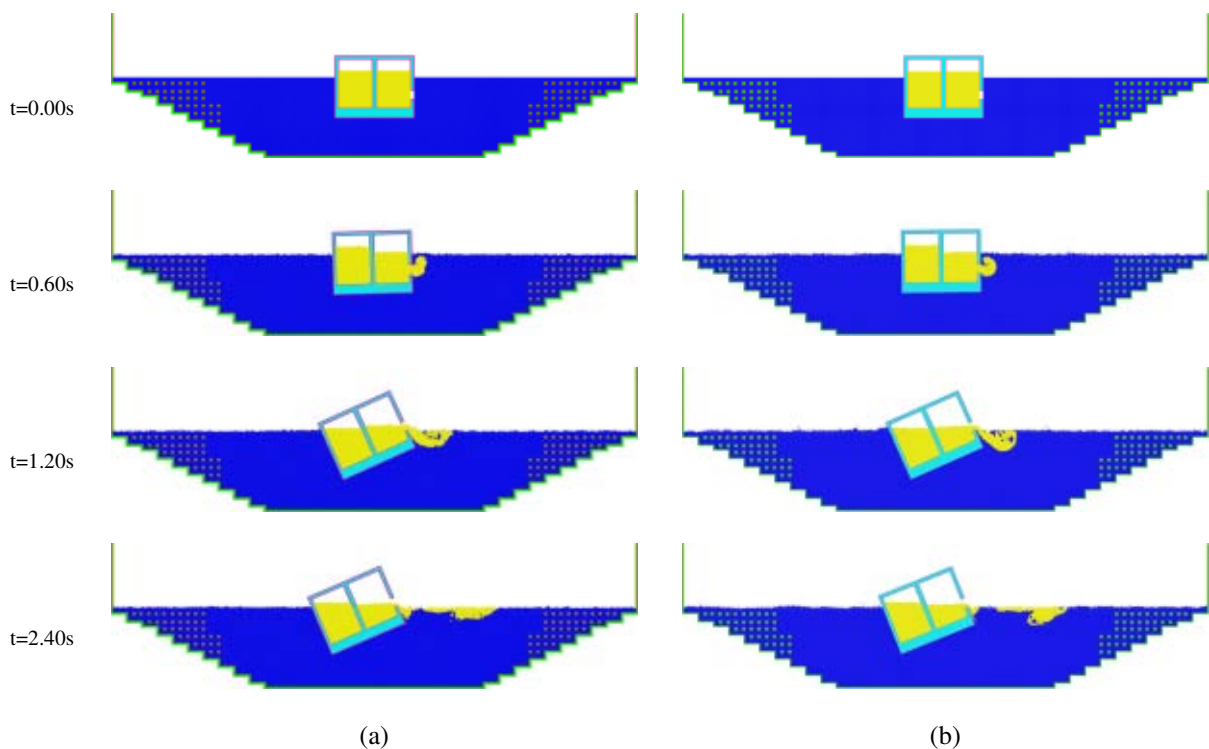


**Figure 5:** Snapshots of the simulations of the case B0\_75%\_010 with low (a) and high (b) resolutions

The validation of final equilibrium angle of list has been carried out by using SSTAB [5]. SSTAB uses hydrostatic theory to calculate the stability of floating bodies with and without free surface effects, and free to pitch and heavy. In order to model the 2D problem, a 3D model of  $B/L=1/100$  with constant cross section and without trim is used in the SSTAB

calculations. Although SSTAB is able to provide an estimate the final list angle through a quasi-static approach, it is unable to take into account the dynamic effects due to oil leakage or water flooding. In this way, the final list angle provided by SSTAB is determined by using the volume obtained by MPS simulation.

Figure 6(a) provides the comparison of the time series of the roll motions obtained by MPS simulation with low and high resolutions, together with the final list angles obtained by SSTAB for the case B0\_75%\_010. The transient motions calculated by MPS show damped oscillations of the motion after quick inclination from the initial position. Despite more detail description of the oil flow outside the hull provided by the simulation with high resolution, the agreement between the time series of the low and high resolutions is very good. This is because the details of the oil flow outside the hull are not relevant for the hull motion and the refinement of the spatial resolution has no effect on the numerical results.

In the case of B0\_75%\_014 (Figure 6(b)), in which the leakage volume and final list are smaller than the former one, the same tendency is observed in despite of the slightly larger discrepancy between the motion time series obtained by the simulations with low and high resolutions. In addition to this, the computed time series of both B0\_75%\_010 and B0\_75%\_014 converge to mean values that agree very well with the final list angles obtained by SSTAB.

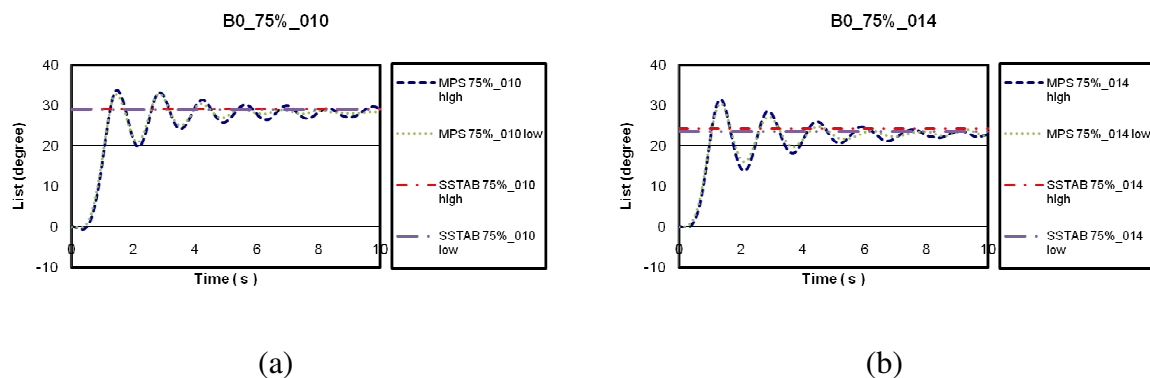


**Figure 6:** Comparison of the time histories of the list angle obtained by transient analysis of MPS and list angle obtained by the hydrostatic analysis of SSTAB showing the effects of resolution in the cases B0\_75%\_010 (a) and B0\_75%\_014 (b)

Figure 7(a) and Figure 7(b) show the time series of the cases B0\_45%\_010 and B0\_45%\_014, respectively. As in the cases with 75% filling, oil leakage occurs. However, as the initial vertical distances between the oil level and the opening are decreased, both the leakage volume and the final list angles are reduced. This might be the reason why the discrepancies between the time series with low and high resolutions occur from the early instants of the simulations.

The snapshots of B0\_45%\_014 presented in Figure 8 show that this is a critical case where very small volume of oil is released and spatial resolution of MPS modeling might affect small simulation results. Also, the drift motion becomes negligible and there are almost no dynamic effects induced by the a relatively small volume of oil leakage.



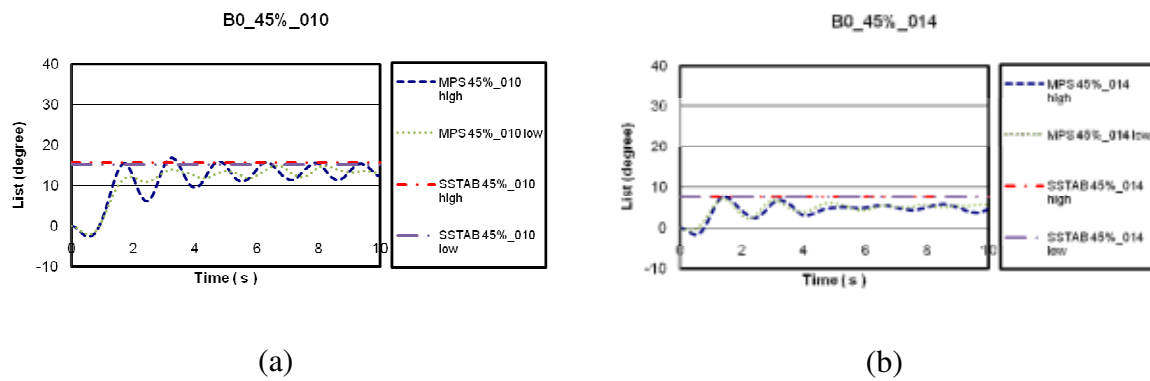


**Figure 7:** Comparison of the time histories of the list angle obtained by transient analysis of MPS and list angle obtained by the hydrostatic analysis of SSTAB showing the effects of resolution in the cases B0\_45%\_010 (a) and B0\_45%\_014 (b)

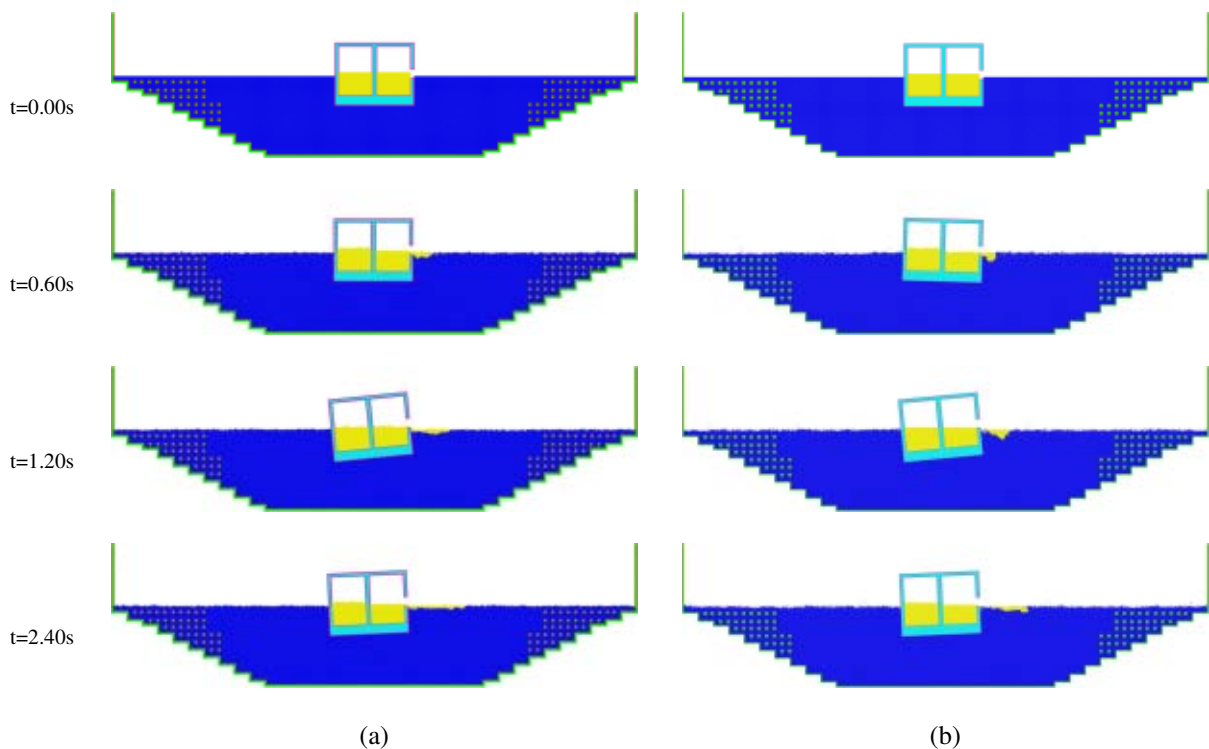


**Figure 8:** Snapshots of the simulations of the case B0\_45%\_014 with low (a) and high (b) resolutions

Figure 9 gives the volume of the oil leakage calculated by MPS, together with the leakage estimate by using SSTAB through quasi-static approach. The vertical axis of Figure 9 is the volume of the leaked oil in relation to the volume of one internal tank. The comparison between the results shows very good agreement. Despite the dynamic effects such as roll and drift motions, the discrepancies are quite small, especially in the cases where the leakage is larger. On the other hand, similar tendency can be observed in the discrepancies between the low and high resolution results. For the case B0\_45%\_014, for example, in which the leakage

is about 8%, the discrepancy due to the spatial resolution achieves 17.5%.

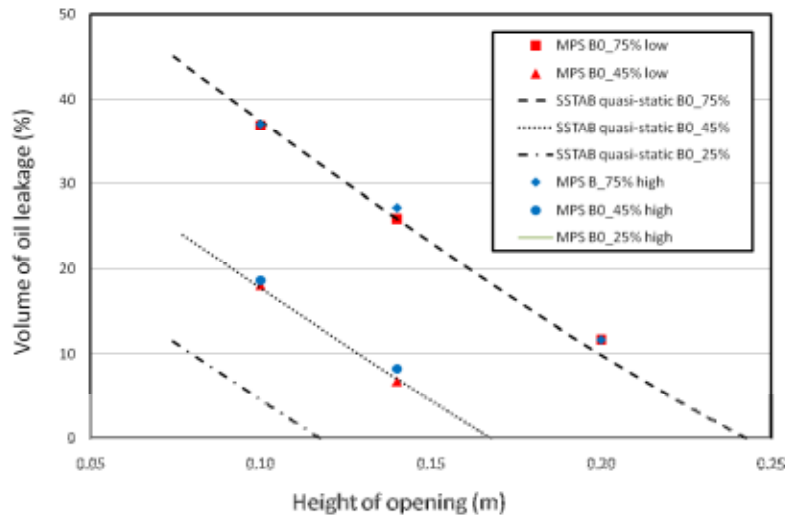
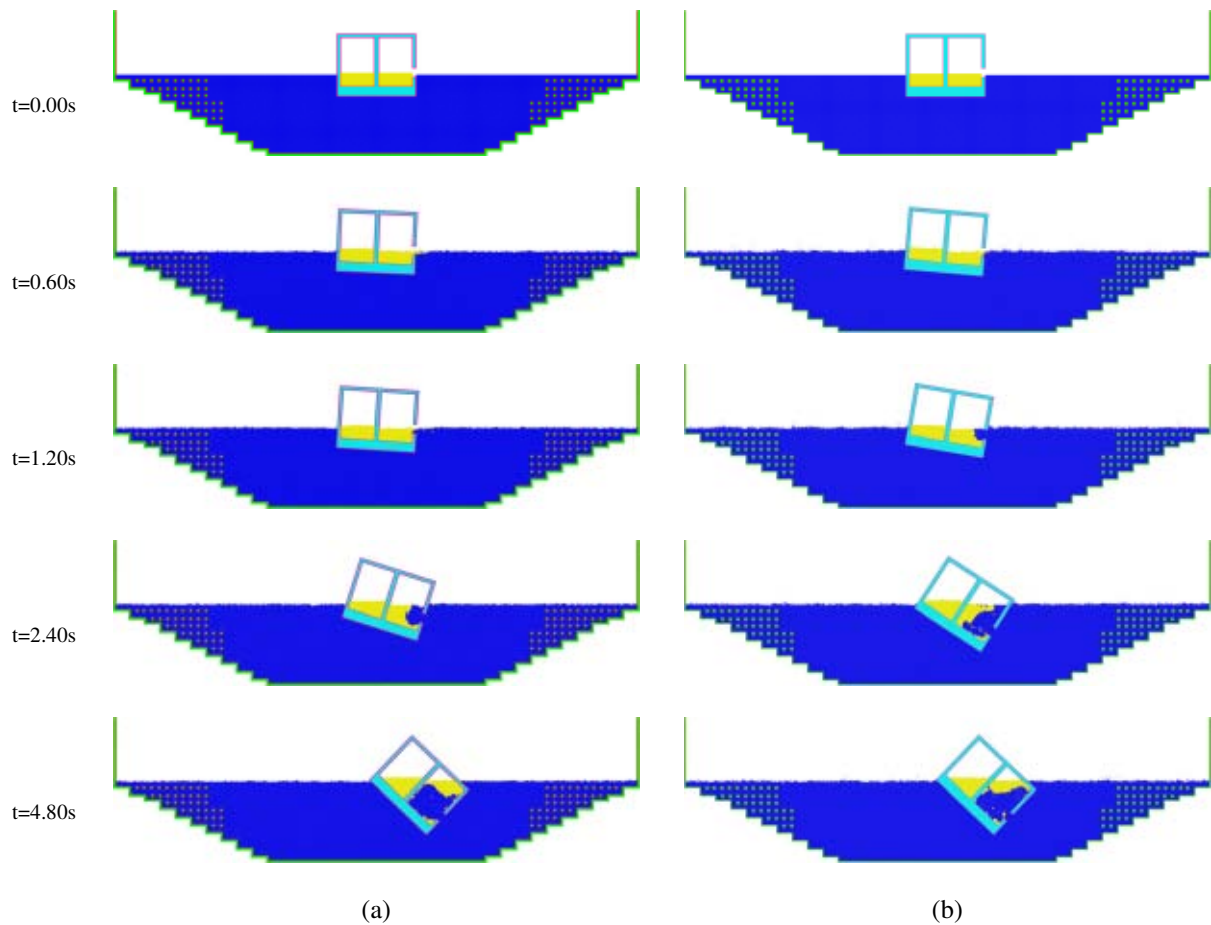


**Figure 9:** Oil leakage obtained by MPS and by quasi-static calculation using SSTAB for 45% and 75% filling and opening height of 0.10 m, 0.14 m and 0.20 m

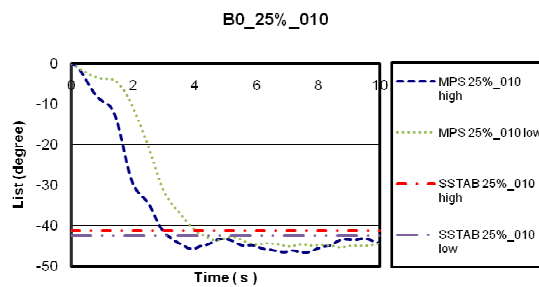
Also, as shown in Figure 9, for filling ratio of 25% (B0\_25%), the quasi-static approach predicts oil leakage when opening height is 0.10 m. This occurs because one of the key assumptions of the quasi-static approach is very small opening. However, as illustrated in Figure 10, which presents the snapshots of the simulation results of B0\_25%\_010, instead of oil leakage, water flooding occurs.

Figure 10 clearly shows how this situation unexpected by quasi-static approach occurs: initially, as the oil and water surface and the opening are almost at same level, after a very shortly oil leakage, increasing volume of water floods into the tank. As the negative list angle increases, water floods quickly into the tank and the final list angle reaches to  $-45^\circ$ . Finally, the flooding water, whose density and surface tension are larger than oil, washes the bottom and inner side walls of the tank and pushes the oil to the tank ceiling. As the void space of the tank is relatively large in this case, a huge amount of water floods into the tank and the final volume of flooded water calculated by MPS is as large as 65.3% of the volume of one internal tank. This huge discrepancy between the results obtained numerical and analytically shows the limit of the validity of the quasi-static approach.

Time series of the cases B0\_25%\_010 is illustrated in Figure 11. The figure shows that the transient motion is strongly affected by the spatial resolution: the roll motion obtained with higher spatial resolution is faster than that obtained with low resolution. As shown in Figure 10, the oil and water flows through a small portion of the opening. In the simulation with low resolution the computed inward and outward flows are smaller because it involves few fluid particles, and most of them are the free surface one, without dynamic pressure.



**Figure 10:** Snapshots of the simulations of the case B0\_25%\_010 with low (a) and high (b) resolutions



**Figure 11:** Comparison of the time histories of the list angle obtained by transient analysis of MPS and list angle obtained by the hydrostatic analysis of SSTAB showing the effects of resolution in the cases B0\_25%\_010

## 5 CONCLUDING REMARKS

In the present paper, a numerical approach based on MPS (Moving particle Semi-Implicit) method is adopted to model the fluid-solid interaction with complex geometry and multiphase oil-water flow to investigate the dynamics of the oil leakage and water flooding in a damaged

crude oil carrier.

The numerical simulations of the transient motion show that the drift motion induced by the leakage may occur in the beginning, when a relatively large volume of oil is released suddenly. From the comparison of the final list angles with that obtained by SSTAB, which is a static stability code, it is clear that the numerical approach is very effective to predict the dynamic behavior of a damaged oil carrier from breakdown to final list, such as damped roll motion and its response time, which might be important for the safeguard issues.

Concerning the accuracy of the numerical results, it increases in cases where the filling ratio is large and the height of the damage is low. The effects of the spatial resolution of the MPS modeling on the accuracy of the numerical results were also analyzed, and it is critical in the case of low filling where the water flooding occurs or when leakage volume is small.

On the other hand, despite the complete simulation of the oil spillage was not realized because the formation of a thin film of oil will demand a very large number of particles that is beyond the scope of the present study, the comparison of the computed oil volume with that obtained by quasi-static approach shows the limit of validity of the last one.

Finally, for sake of simplicity, 2D modeling was carried out to investigate the complex fluid-solid interaction phenomena. This is a hypothetical situation in which the dimension of the damage is much larger than the actual cases. In this way, instead of extrapolating straightforwardly the 2D results to the actual situations, further complete 3D analysis should be done. In addition to this, future works on the effects of the air inside the tank are also required.

## ACKNOWLEDGMENTS

The author would like to express their gratitude to PETROBRAS for the financial support to the research.

## REFERENCES

- [1] Koshizuka, S. and Oka, Y. Moving-particle semi-implicit method for fragmentation of incompressible fluid. *Nuclear Science and Engineering*, 123:421–434, (1996).
- [2] Kondo, M., Koshizuka, S., Takimoto, M. Surface tension model using inter-particle potential force in Moving Particle Semi-implicit method. *Transactions of JSCEs*, paper No. 20070021, (2007).
- [3] Cheng, L. Y., Gomes, D. V., Nishimoto, K. A numerical study on oil leakage and damaged stability of oil carrier. In: *The Proceedings of the 29th International Conference on Offshore Mechanics and Arctic (OMAE'2010)*, Jun. 2010, Shanghai, China. Paper No. OMAE2010-20827.
- [4] Cheng, L. Y., Gomes, D. V., Yoshino, A. M., Nishimoto, K. A numerical study on water flooding in a damaged oil carrier. In: *The Proceedings of the 30th International Conference on Offshore Mechanics and Arctic (OMAE'2010)*, Jun. 2010, Rotterdam, Netherland. Paper No. OMAE2011-49616.
- [5] Coelho, L.C.G., Nascimento, A.A. – *SSTAB User's Manual*, PUC, Tecgraf, (2003).